Electrochemical properties of cross-linked polymer electrolyte by electron beam irradiation and application to lithium ion batteries

M. Ueno, N. Imanishi*, K. Hanai, T. Kobayashi, A. Hirano, O. Yamamoto, Y. Takeda

Department of Chemistry for Materials, Graduate School of Engineering, Mie University, 1577 Kurimamachiya-cho, Tsu, Mie 514-8507, Japan

ARTICLE INFO

ABSTRACT

A polymer electrolyte was successfully fabricated for a room temperature operation lithium battery by cross-linking the mixture of oligomeric poly (ethylene glycol) dimethylether (PEGDME) and poly (ethylene glycol) diacrylate (PEGDA) with $Li(CF_3SO_2)_2N$ using electron beam irradiation. The maximum ionic conductivity achieved for the cross-linked solid polymer electrolyte (c-SPE) at room temperature was $2.1 \times 10^{-4} \, S \, cm^{-1}$ and the lithium transport number of the electrolyte was around 0.2. The c-SPE showed no reaction heat with lithium metal up to 300 °C. The interface resistance of Li/c-SPE/Li at room temperature was about $45 \, \Omega \, cm^2$, which is considerable lower than that of $210 \, \Omega \, cm^2$ for $Li/PEO_{10}Li(CF_3SO_2)_2N/Li$. The electrochemical window of the polymer electrolyte was above 4 V (versus Li^+/Li). The initial discharge capacity for the $Li/SPE/LiFePO_4$-C cell was approximately $90 \, mAh \, g^{-1}$ for $LiFePO_4$-C at 1/10 °C rate at room temperature and showed a good cyclability and a high coulombic efficiency of 99.2%.

1. Introduction

With increasing motorization, electric vehicles have become more important to address environmental issues. Lithium ion batteries are one of the most appropriate power sources for electric vehicles. Currently, lithium ion batteries with a liquid electrolyte are mainly applied in portable devices. The battery includes a flammable organic solvent that has the risk of ignition, so that scaling up for larger applications is hazardous. Various technologies have been developed to achieve nonflammable and safe lithium ion batteries. Wright et al. discovered ionic conduction in the complexes of poly(ethylene oxide) (PEO) and alkaline salts [1], and since then the solid polymer electrolyte (SPE) has attracted much attention due to its flexibility and thermal stability. PEO has been the most widely used host polymer in typical dry SPEs. However, these SPEs have a critical problem in that the conductivity drops steeply around room temperature, as a result of crystallization of the host polymer [2,3]. To solve this problem, various strategies have been proposed. Fan and Fedkiw [4] reported composite electrolytes prepared from fumed silica, polyethylene oxide oligomer and lithium salts, which exhibited a high conductivity of $1.5 \times 10^{-3} \, S \, cm^{-1}$ at room temperature. They exhibit a gel-like consistency but flow under shear. Abraham et al. studied a composite polymer electrolyte that consisted of a poly(vinylidene

fluoride)–hexafluoropropene (PVdF–HFP) framework plasticized with a solution of lithium salt in oligomeric poly(ethylene glycol) dimethyl ether (PEGDME), which exhibited practical conductivities at lower temperatures [5]. Choi et al. investigated a composite polymer electrolyte that consisted of PEO and an ionic liquid, in which improvement of the ionic conductivity was accomplished at ambient temperature [6]. On the other hand, cross-linking is an effective way to suppress crystallization and is also beneficial to enhance the mechanical strength of the polymer. Kang et al. examined a cross-linked polyacrylate electrolyte incorporated with PEGDME by curing with ultraviolet radiation [7]. And Maccallum et al. [8] and Kronfli et al. [9] have reported the cross-linking of PEO-LiX by γ-radiation. However, such light or thermal cross-linking generally requires additional chemicals to make the reaction occur smoothly, and these additives may have a negative influence in battery applications, and γ-radiation needs a Co-60 source.

Cross-linking of polymers using electron beam (EB) irradiation has many advantages, such as shortening of the reaction time, initiator-free polymerization, ease of changing the dose and high uniformity of the cross-linking level [10]. As an example of this technique applied to the battery field, we reported that EB irradiation to cross-link the PEO electrolyte resulted in the inhibition of crystallization [11]. However, crystallization of the polymer was not completely inhibited and the ionic conductivity at room temperature was not significantly improved. Two main observations from these results were obtained; (1) it is impossible to prevent crystallization by cross-linking part of the long polymer chain, and (2) the ionic mobility of the polymer is

* Corresponding author. Tel.: +81 59 231 9420; fax: +81 59 231 9478.
 E-mail address: imanishi@chem.mie-u.ac.jp (N. Imanishi).

Table 1
Experimental conditions.

Parameter	Condition
PEGDME, M_w	250, 500, 1000, 8000
PEO, M_w	1×10^5, 6×10^5
Lithium ion concentration/Li/O	1/6, 1/10, 1/18, 1/36, 1/54
EB irradiation dose/kGy	30, 60, 90, 180, 270
Molar ratio of PEGDME (or PEO)/(PEGDA)	4/1, 2/1, 1/1, 1/2, 1/4

decreased by further cross-linking. The purpose of this study is to develop the thermal stable lithium conducting polymer electrolyte with high conductivity at room temperature. Cross-linked solid polymer electrolytes (c-SPE) were investigated and consisted of oligomeric PEGDME (Mw < 2000) and poly(ethylene glycol) diacrylate (PEGDA) as a cross-linking aid for EB irradiation. The solid phase content, ionic conductivity, lithium ion transport number, thermal behavior, lithium/SPE interfacial property and charge-discharge performance were examined as a function of the molecular weight of PEGDME and lithium ion concentrations of c-SPE.

2. Experimental

2.1. Sample preparation

PEGDME (M_w = 250, 500, 1000, Aldrich), PEO (M_w = 8000, 1×10^5, 6×10^5), PEGDA (M_w = 575, Aldrich) and Li(CF$_3$SO$_2$)$_2$N (LiTFSI; Wako chemicals) were used as purchased. c-SPEs were prepared by the casting method in an argon-filled glove box. Specific amounts of PEGDME (or PEO), PEGDA and LiTFSI were mixed and stirred at 300 rpm for 6 h, followed by casting of the mixture on a copper foil. The film was cross-linked using EB irradiation at various irradiation doses in a nitrogen atmosphere at an accelerating voltage of 220 kV. The c-SPE films were then completely dried in a vacuum oven at 90 °C for 10 h. The preparation conditions are summarized in Table 1. PEO$_{10}$LiTFSI (M_w = 6×10^5 and 10^5) for comparison to cross-linked PEGDME was obtained by the casting method [12] and cross-linked by EB radiation.

2.2. Measurements

The ionic conductivity of the SPEs was evaluated using the Cu/SPE/Cu symmetrical cell. Ac impedance of the samples was measured in the frequency range of 1 MHz–1 Hz using a Solartron 1260 impedance analyzer from 0 to 60 °C. The lithium ion transport number at 60 °C was estimated by Eq. (1) [13].

$$\tau_{Li^+} = \frac{I_s(\Delta V - I_0 R_i^0)}{I_0(\Delta V - I_s R_i^s)} \tag{1}$$

where ΔV is the applied DC voltage (in this case, ΔV = 10 mV), I_0 is the initial current measured at the point that DC voltage is applied, R_i^0 is the initial lithium interfacial resistance, I_s is the steady state current, and R_i^s is the lithium interfacial resistance at steady state.

The solid phase content of c-SPE by EB irradiation was evaluated from the amount of weight change of c-SPE before and after immersion in acetonitrile (AN) for 3 days and vacuum drying at 90 °C for 10 h. The content was calculated using Eq. (2).

$$\text{Solid phase content(wt\%)} = \frac{\text{weight (after drying)}}{\text{weight (before immersion in AN)}} \times 100 \tag{2}$$

The thermal properties of SPE were measured using differential scanning calorimetric analysis (DSC) using a Rigaku DSC 8230 and thermogravimetric/differential thermal analysis (TG/DTA) using a Rigaku TG 8120 in the range from 20 to 600 °C with a heating rate of 5 °C min^{-1} in an air atmosphere.

Cyclic voltammetry was measured at 20 °C using a Li/SPE/M (M = Au, Al) cell configuration at a sweep rate of 5 mV s^{-1}. Charge–discharge performance was measured galvanostatically at 20 °C with a C/10 rate using a charge–discharge measurement system (Nagano). A carbon-coated LiFePO$_4$ (LiFePO$_4$-C) was used as the cathode active material (AM), and vapor grown carbon fiber (VGCF, Showa Denko) as a conductive agent. The weight ratio of AM:VGCF:SPE was 56:14:30. A mixture of the components in AN was cast on aluminum foil with an applicator. The film was cross-linked by EB irradiation at a dose of 270 kGy in a nitrogen atmosphere at an accelerating voltage of 220 kV. After vacuum drying at 90 °C for 10 h, the LiFePO$_4$-C/SPE/Li half cell was constructed.

3. Results and discussion

The solid phase content in the c-SPE as a function of EB irradiation dose is shown in Fig. 1. The molar ratio of PEGDME (M_w = 500) (PEGDME-500) and PEGDA (M_w = 575) was 2/1 and the content of LiTFSI in the SPE was Li/O = 1/10. A self-supported film was formed for an irradiation dose over 60 kGy. In contrast to the significant decrease in the solid phase content with an EB irradiation dose below 60 kGy, higher doses increase the solid phase content only moderately, up to approximately 70% at 270 kGy. EB irradiation results in the simultaneous cross-linking and scission of the polymer chain. The balance of these two processes determines the final solid phase content. The weight of the polymer residue after immersion in AN and vacuum drying was always much heavier than the amount of PEGDA used for each condition, which indicates that cross-linking occurred not only between PEGDA molecules, but also between PEGDA and PEGDME.

Table 2 shows the solid phase contents of c-SPEs prepared from PEGDME–PEGDA with various molecular weight and differ-
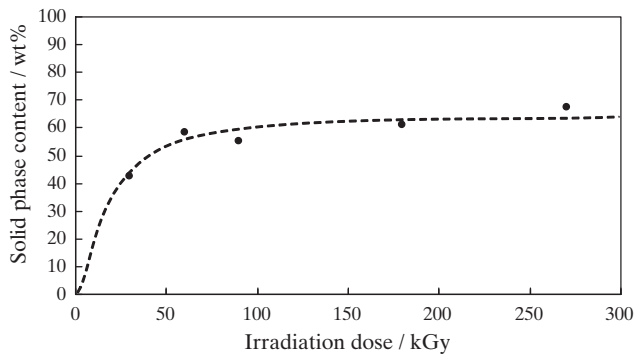
Table 2
Solid phase contents of cross-linked PEGDME–PEGDA.

M_w (PEGDME)	Molar ratio (PEGDME/PEGDA)	Solid phase content (%)	M_w (PEGDME)	Molar ratio (PEGDME/PEGDA)	Solid phase content (%)
250	4/1	60.2	1000	4/1	–
	2/1	72.3		2/1	40.1
	1/1	90.2		1/1	60.0
	1/2	92.2		1/2	70.6
	1/4	89.6		1/4	86.2
500	4/1	49.4	2000	4/1	–
	2/1	67.5		2/1	–
	1/1	76.0		1/1	–
	1/2	86.6		1/2	64.8
	1/4	93.8		1/4	78.1

Not self supported film, Li ion concentration: Li/O = 1/10.

Fig. 1. Solid phase contents in a cross-linked PEGDME ($M_w = 500$)-PEGDA ($M_w = 575$)–LiTFSI (Li/O = 1/10) as a function of EB irradiation dose, where PEGDME/PEGDA = 2/1.

Table 3
Li$^+$ transport numbers for cross-linked PEGDME-PEGDA and non-cross-linked PEO.

Materials	M_w	Lithium ion transport number
Cross-linked PEGDME–PEGDA	250	0.19
	500	0.19
	1,000	0.19
Non-cross-linked PEO	6×10^5	0.17

Li ion concentration: Li/O=1/10.

ent amounts of PEGDA at an EB irradiation dose of 270 kGy. The lithium ion concentration was fixed as Li/O = 1/10. The solid phase content decreased gradually with decreasing amount of PEGDA, and the c-SPE could not maintain a self-supporting state with a solid phase content of below approximately 40%. Using PEGDME with higher molecular weight also resulted in a decrease of the solid state content with decreasing amount of PEGDA.

Fig. 2(a) shows Arrhenius plots for the ionic conductivity of cross-linked PEGDME–PEGDA (2:1 molar ratio) and PEO–PEGDA (2:1 molar ratio) at an EB irradiation dose of 270 kGy, where Li/O is 1/10. For higher molecular weight cross-linked PEO, the knees in the conductivity plot shifted toward slightly lower temperatures compared to non cross-linked PEO, while the cross-linked PEGDME-1000-PEGDA shows a conductivity knee at about 14 °C and that with oligomeric PEGDME-500 and PEGDME-250 shows no clear conductivity knee to 0 °C. The ionic conductivity for c-SPE with PEGDME-250 was 2.1×10^{-4} S cm^{-1} at 20 °C, which is one order higher than that for cross-linked PEO ($M_w = 6 \times 10^5$). The conductivity of the cross-linked PEO–PEGDA is lower than that of PEO$_{10}$LiTFSI of which conductivity plot is shown in Fig. 2(b). The low conductivity of the cross-linked PEO may be due to the rigid matrices. Fig. 2(b) shows Arrhenius plots for the ionic conductivity of cross-linked PEGDME-500-PEGDA and non-cross-linked PEO ($M_w = 6 \times 10^5$) with different salt concentrations (Li/O = 1/10, 1/18). The ionic conductivity of the cross-linked PEGDME–PEGDA and high temperature melt phase of PEO shows no dependence on the concentration of LiTFSI. While, the low temperature solid phase of PEO shows significant dependence on concentration of the lithium salt. These results suggest that the high conductivity near room temperature of the cross-linked PEGDME–PEGDA could be explained by existence of a liquid phase in the cross-linked matrix.

Fig. 3 shows the lithium ion transport number dependence on salt concentration for the cross-linked PEGDME-500-PEGDA-LiTFSI and non-cross-linked PEO$_x$LiTFSI ($M_w = 6 \times 10^5$). The lithium ion transport numbers are in a range of 0.1–0.2 for both samples. Table 3 summarizes the transport numbers obtained for c-SPE with different molecular weight of PEGDME and PEO$_{10}$LiTFSI.

Fig. 4 shows the thermal properties of c-SPE with different molecular weight PEGDME, where Li/O is 1/10 and non-cross-

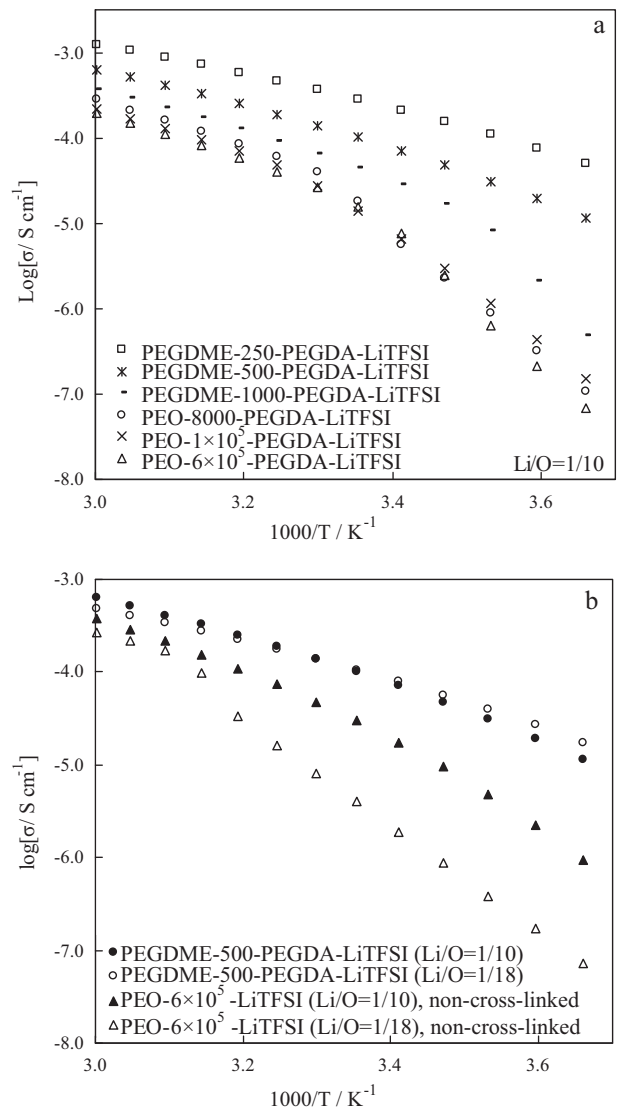**Fig. 2.** Arrhenius plots of ionic conductivity (a) for cross-linked PEGDME/PEGDA ($M_w = 575$) (2/1 weight ratio)–LiTFSI (Li/O = 1/10) with various molecular weight of PEGDA and cross-linked PEO$_{10}$LiTFSI, and (b) for cross-linked PEGDME ($M_w = 500$)/PEGDA = 2/1] and non-cross-linked PEO ($M_w = 6 \times 10^5$) as a function of lithium ion concentration.
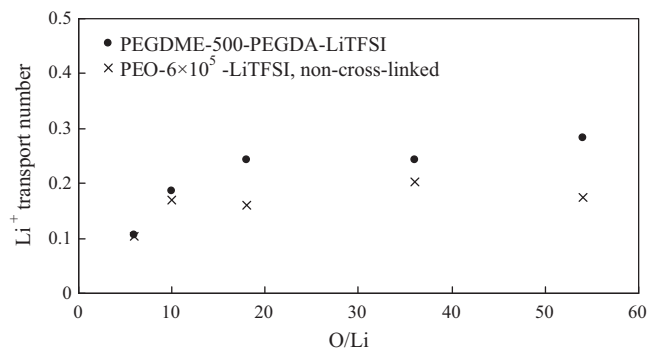

Fig. 3. Li$^+$ transport number for cross-linked PEGDME ($M_w = 500$)/PEGDA (2/1)–LiTFSI and non-cross-linked PEO$_{10}$ ($M_w = 6 \times 10^5$) LiTFSI as a function of lithium ion concentration.
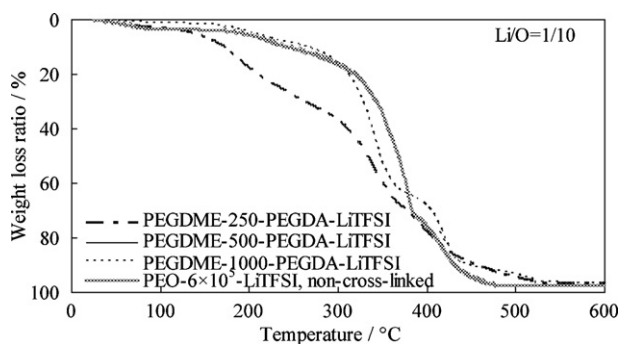
Fig. 4. TGA curves for cross-linked PEGDME/PEGDA (2/1)–LiTFSI (Li/O = 1/10) and non-cross-linked PEO$_{10}$ ($M_w = 6 \times 10^5$) LiTFSI.

Fig. 6. DSC curves of cross-linked PEGDME ($M_w = 500$)/PEGDA (2/1)–LiTFSI (Li/O = 1/10) mixed with Li metal and EC/DEC (1/1 vol. ratio)-1 M LiPF$_6$ mixed with Li metal.

linked PEO$_{10}$LiTFSI. Three distinctive weight loss steps were observed in the TGA profiles, as shown in Fig. 4, and are characterized as follows. The first step (ca. 180 °C) indicates evaporation of free low molecular weight PEGDME and PEGDA, the second step (ca. 300 °C) indicates the decomposition of cross-linked PEGDME–PEGDA or PEO, and the third step (ca. 400 °C) indicates the decomposition of LiTFSI. The first weight loss temperature at ca. 180 °C were almost similar, regardless of the molecular weight of PEGDME, but the weight loss ratios were higher for PEGDMEs with $M_w = 250$ and 500. This is because these samples contain about 40% of an AN soluble phase as shown in Fig. 1. Fig. 5 shows molecular weight distribution of soluble components in AN from the cross-linked PEGDME-500-PEGDA, which is compared to that of PEGDME. The both molecular weight distributions are similar and the formation of short chain oligomers is not observed by the EB radiation.

Fig. 6 shows DSC profiles of the mixture of cross-linked PEGDME-500-PEGDA-LiTFSI (Li/O = 1/10) and lithium metal along with the mixture of ethylene carbonate/diethyl carbonate (1/1 vol.
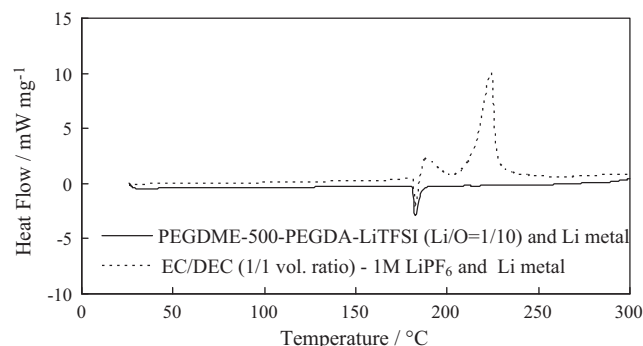
ratio) with LiPF$_6$ and lithium metal. The endothermic peaks are observed at around 180 °C in both profiles. This peak is caused by melting of lithium metal. A distinctive difference of the profiles confirms the thermal stability for the cross-linked PEGDME–PEGDA. The liquid electrolyte and lithium metal mixture shows a reaction heat, but the cross-linked PEGDME–PEGDA and lithium metal show no reaction peak up to 300 °C. This result indicates that the self-supported cross-linked PEGDME–PEGDA with a high ionic conductivity at room temperature is more safety compared to the conventional liquid electrolyte.

Generally, lithium ion conducting polymer electrolyte showed a high interfacial resistance between lithium metal and polymer electrolyte by a formation of passivation layer [14]. And in some examples the interfacial resistance increased with time [15]. Fig. 7(a) shows Cole-Cole plots of Li/cross-linked PEGDME-500-PEGDA-LiTFSI (Li/O = 1/10)/Li and Li/PEO$_{10}$LiTFSI ($M_w = 6 \times 10^5$)/Li as a function of the storage time at 60 °C. The impedance profiles of Li/PEO$_{10}$LiTFSI/Li show a small semicircle in a high frequency range and a large semicircle in a low frequency range. The high frequency range semicircles could be assigned as the grain boundary resistance of the polymer electrolyte. The large semicircle is associated with the overall interface resistance, which consists of the interface resistance of the passivation layer and the charge transfer resistance [16]. The Li/cross-linked PEGDME-500-PEGDA-LiTFSI (Li/O = 1/10)/Li cell shows a little different impedance profile to that of PEO$_{10}$LiTFSI. The high frequency semicircle is larger than that of PEO$_{10}$LiTFSI and the total cell resistance is almost half of that of PEO$_{10}$LiTFSI. The high frequency semicircle could be assigned to a kind of bulk resistance and the low frequency semicircle is assigned to the passivation layer and the charge transfer resistance, because the high frequency intercept of the low frequency semicircle with the real axis hardly changes with the storage period compared to that of the low frequency intercept. The storage time dependences of interface resistance at 60 °C of Li/cross-linked PEGDME-500-PEGDA-LiTFSI (Li/O = 1/10)/Li and Li/PEO$_{10}$LiTFSI ($M_w = 6 \times 10^5$)/Li are shown in Fig. 7(b). The cross-linked PEGDME–PEGDA shows a low and stable interface resistance. The specific interface resistance at 60 °C of 40.5 Ω cm^2 is compared to that of the recently reported low interface specific resistance of about 100 Ω cm^2 [16]. The low specific resistance is quite attractive for the electrolyte in lithium batteries with lithium anode.

The electrochemical stability of the electrolyte is an important requirement for the electrolyte in batteries. Fig. 8 shows cyclic voltammograms of Li/cross-linked PEGDME-500-PEGDA-LiTFSI (Li/O = 1/10)/Au and Li/PEO ($M_w = 6 \times 10^5$)$_{10}$LiTFSI/Au. In the anodic scan in the both cells, the oxidation peak corresponding to electrolyte decomposition appears at around 4.5 V (vs. Li$^+$/Li). From an enlarged scale current axis, the oxidation current began to occur at approximately 4 V and increased significantly at 4.5 V. It has been
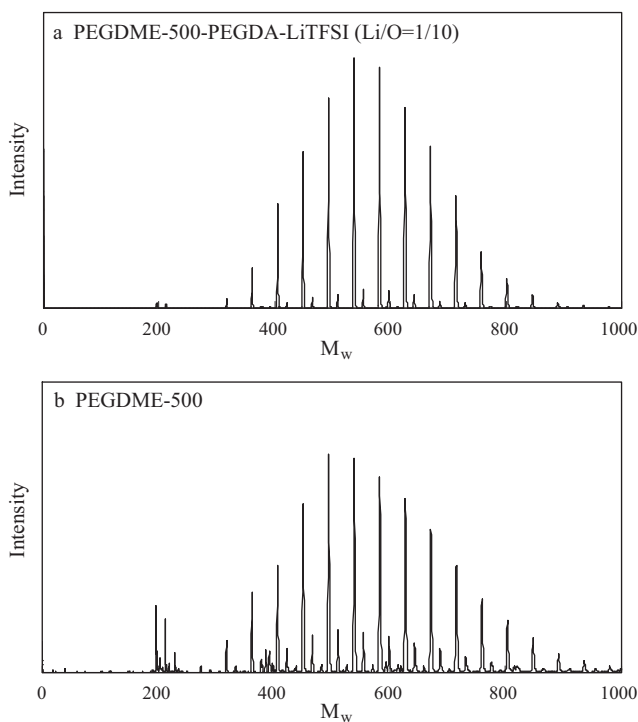

Fig. 5. Molecular weight distribution of (a) soluble component in AN of cross-linked PEGDME ($M_w = 500$)/PEGDA (2/1)–LiTFSI (Li/O = 1/10) and (b) liquid PEGDME ($M_w = 500$).
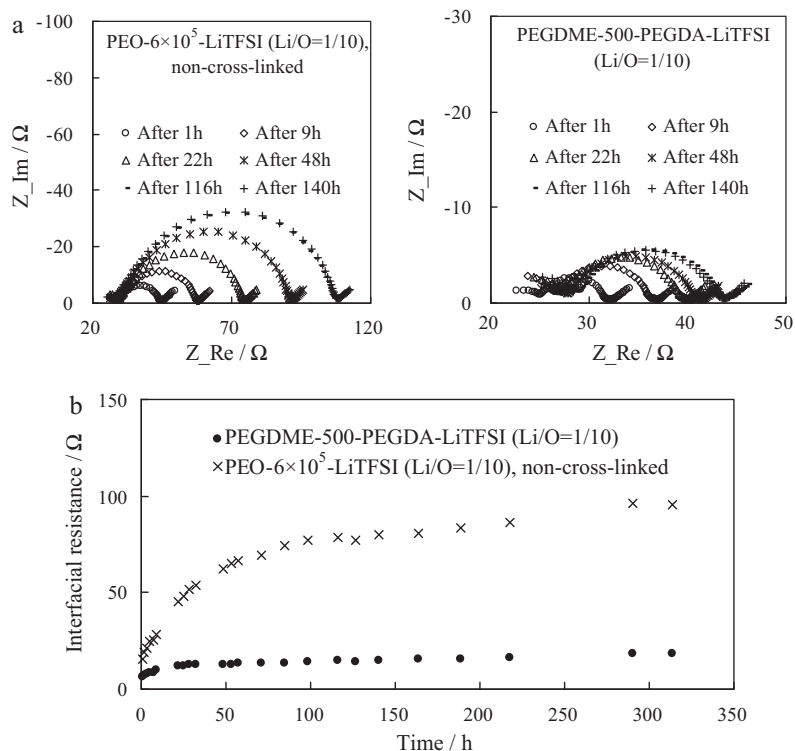
Fig. 7. Impedance profiles of (a) Li/PEO$_{10}$ ($M_w = 6 \times 10^5$)LiTFSI/Li and Li/cross-linked PEGDME ($M_w = 500$)/PEGDA (2/1)–LiTFSI (Li/O = 1/10) at 60 °C, and (b) time dependence of the interfacial resistances.

reported that oxidation of the PEO-based polymer starts at around 4 V [17]. The peak current for the cross-linked PEGDME–PEGDA electrolyte is higher than that for the non-cross-linked PEO. This is due to the higher kinetics of polymer decomposition in the former and we consider that the oxidation potentials are essentially the same for both electrolytes. The redox potential of the LiFePO$_4$ positive electrode in common use is 3.5 V; therefore, it is safe to use with this cross-linked electrolyte. On the reduction side, deposition and dissolution of lithium ions occur on the working electrode at approximately 0 V. No other peaks that would indicate side reactions were observed. In the c-SPE, a larger reversible current flowed at 0 V, which is also attributed to the faster ionic mobility in c-SPE. This result is in good agreement with the small interfacial resistance shown in Fig. 7.

To demonstrate the applicability of the cross-linked electrolyte in lithium cells, the charge–discharge performance of Li/cross-linked PEGDME-500-PEGDA/LiFePO$_4$ was tested and com-

pared to that of Li/PEO$_{10}$LiTFSI/LiFePO$_4$. Fig. 9(a) shows the first charge–discharge curves at 20 °C with C/10 rate. A capacity of approximately 90 mAh g^{-1} was obtained for the c-SPE, however, that for PEO$_{10}$LiTFSI was only 30 mAh g^{-1}. The cycling properties

Fig. 9. (a) The first cycle charge–discharge properties for Li/cross-linked PEGDME ($M_w = 500$)/PEGDA(2/1)–LiTFSI (Li/O = 1/10)/LiFePO$_4$ and Li/PEO$_{10}$($M_w = 6 \times 10^5$)LiTFSI/Li at 20 °C and at 1/10 rate, and (b) the cycling performance of Li/cross-linked PEGDME ($M_w = 500$)/PEGDA(2/1)–LiTFSI (Li/O = 1/10)/LiFePO$_4$ at 20 °C and at 1/10 rate.
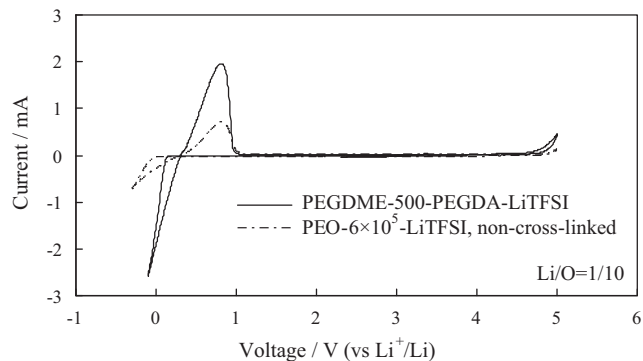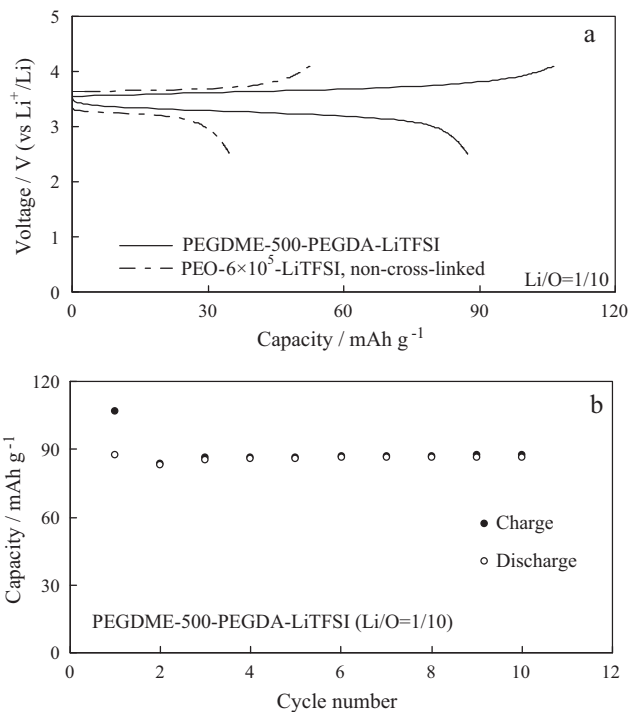

Fig. 8. Cyclic voltammograms for the cross-linked PEGDME ($M_w = 500$)/PEGDA (2/1)–LiTFSI (Li/O = 1/10) and non-cross-linked PEO$_{10}$ ($M_w = 6 \times 10^5$)LiTFSI at 20 °C with a sweep rate of 5 mV s^{-1}.

(Fig. 9(b)) indicated good cyclability for the cell with the c-SPE with an average columbic efficiency of 99.2% at the 2nd and following cycles. These preliminary cell performances suggest that lithium cells with the c-SPE could be used under ambient conditions.

4. Conclusions

A solid polymer electrolyte for room temperature operation lithium batteries was successfully prepared using an electron beam cross-linking technique for the mixture of PEGDME and PEGDA with LiTFSI. The electrolyte consists of cross-linked polymer network with a liquid oligomer. The cross-linked solid polymer electrolyte showed a high ionic conductivity of 10^{-4} S cm^{-1} at room temperature and a good mechanical property. The interface resistance between lithium metal and the cross-linked polymer electrolyte was not so high as observed in lithium metal and the conventional polymer electrolyte of PEO-LiTFSI. The cell with the lithium anode, the cross-linked polymer electrolyte, and the LiFePO$_4$ cathode showed an excellent charge–discharge performance at room temperature.

Acknowledgements

References

[1] D.E. Fenton, J.M. Parker, P.V. Wright, Polymer 14 (1973) 589.
[2] C. Berthier, W. Gorecki, M. Minier, M.B. Armand, J.M. Chabagno, P. Rigaud, Solid State Ionics 11 (1983) 91.
[3] M. Armand, M. Chabagno, M.J. Duclot, in: P. Vashishta, J.N. Mundy, G.K. Shenoy (Eds.), Fast Ion Transport in Solids, North-Holland, Amsterdam, 1979.
[4] J. Fan, P.S. Fedkiw, J. Electrochem. Soc. 144 (1997) 399.
[5] K.M. Abraham, Z. Jiang, B. Carroll, Chem. Mater. 9 (1997) 1978.
[6] J.W. Choi, G. Cheruvally, Y.H. Kim, J.K. Kim, J. Manuel, P. Raghavan, J.H. Ahn, K.W. Kim, H.J. Ahn, D.S. Choi, C.E. Song, Solid State Ionics 178 (2007) 1235.
[7] Y. Kang, H.J. Kim, E. Kim, B. Oh, J.H. Cho, J. Power Sources 92 (2001) 255.
[8] J.R. Maccallum, M.J. Smith, C.A. Vincent, Solid State Ionics 11 (1984) 307.
[9] E. Kronfli, K.V. Lovell, A. Hooper, R.J. Neat, Br. Polym. J. 20 (1988) 275.
[10] J.P. Collier, B.H. Currier, F.E. Kennedy, J.H. Currier, G.S. Timmins, S.K. Jackson, R.L. Brewer, Clin. Orthop. Relat. Res. 414 (2003) 289.
[11] R. Uchiyama, K. Kusagawa, K. Hanai, N. Imanishi, A. Hirano, Y. Takeda, Solid State Ionics 180 (2009) 205.
[12] K. Hanai, T. Maruyama, N. Imanishi, A. Hirano, Y. Takeda, O. Yamamoto, J. Power Sources 178 (2008) 789.
[13] J. Evans, C.A. Vincent, P.G. Bruce, Polymer 28 (1987) 2324.
[14] G.B. Appetecchi, F. Croce, G. Dautzenberg, M. Mastragostino, F. Ronci, B. Scrosati, F. Soavi, A. Zanelli, F. Alessandrini, P.P. Prosini, J. Electrochem. Soc. 145 (1998) 4126.
[15] Q. Li, T. Itoh, N. Imanishi, A. Hirano, Y. Takeda, O. Yamamoto, Solid State Ionics 159 (2003) 97.
[16] S. Liu, N. Imanishi, T. Zhang, A. Hirano, Y. Takeda, O. Yamamoto, J. Yang, J. Electrochem. Soc. 157 (2010) A1092.
[17] Y.T. Kim, E.S. Smotkin, Solid State Ionics 149 (2002) 29.